microPublication BIOLOGY

11/1/2024 - *Open Access*

Human *SVIP* is sufficient to stimulate tubular lysosomes and extend healthspan in well-fed *Caenorhabditis elegans*

Joshua P. Gill[1], Kathryn R. DeLeo[1], K. Adam Bohnert[1], Alyssa E. Johnson[1§]

[1]Biological Sciences, Louisiana State University, Baton Rouge, Louisiana, United States

[§]To whom correspondence should be addressed: johnsona@lsu.edu

Abstract

Small VCP Interacting Protein (SVIP) is essential for maintaining a unique form of tubular lysosomes (TLs) in *Drosophila*. Although *Caenorhabditis elegans* do not have an annotated *SVIP* ortholog, expression of *Drosophila SVIP* in the *C. elegans* intestine induces TLs constitutively, increases autophagic activity, and extends healthspan. Here, we find that expression of the human ortholog of *SVIP* in the *C. elegans* gut causes similar physiological and phenotypic effects as *Drosophila SVIP*, albeit some effects were less pronounced. These results demonstrate that human *SVIP* can induce functional TLs in *C. elegans* but may be a weaker allele compared to *Drosophila SVIP*.

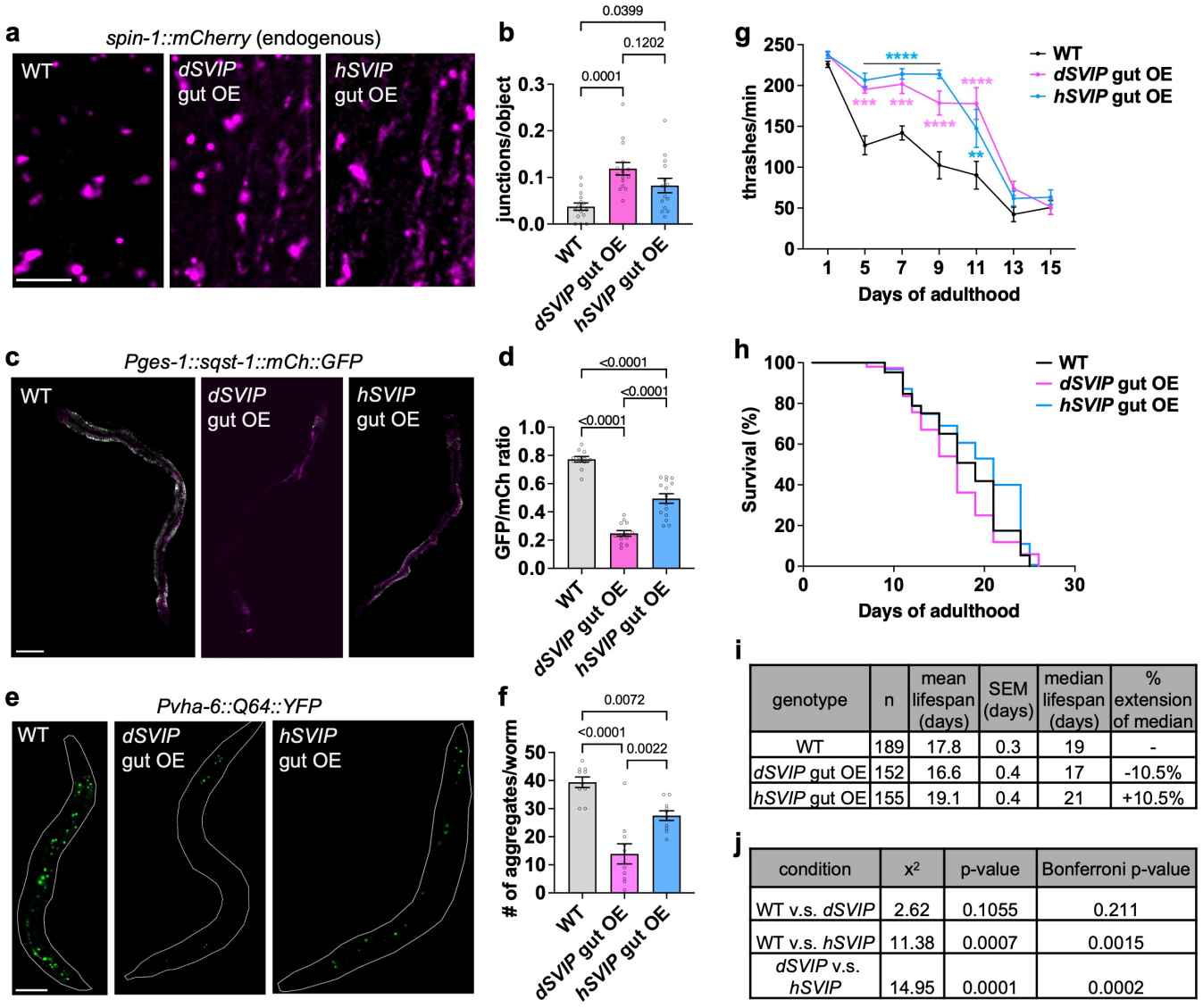

i

genotype	n	mean lifespan (days)	SEM (days)	median lifespan (days)	% extension of median
WT	189	17.8	0.3	19	-
dSVIP gut OE	152	16.6	0.4	17	-10.5%
hSVIP gut OE	155	19.1	0.4	21	+10.5%

j

condition	x^2	p-value	Bonferroni p-value
WT v.s. *dSVIP*	2.62	0.1055	0.211
WT v.s. *hSVIP*	11.38	0.0007	0.0015
dSVIP v.s. *hSVIP*	14.95	0.0001	0.0002

Figure 1. Human *SVIP* induces TLs constitutively, increases autophagic activity, and improves healthspan when expressed in the *C. elegans* gut:

a. Endogenously tagged SPIN-1::mCherry in fed adult day 1 WT, *dSVIP* gut OE, and *hSVIP* gut OE worms (scale bar, 5µm). **b.** Quantification of lysosomal junctions/object in fed adult day 1 WT (n=15 worms), *dSVIP* gut OE (n=15 worms), and *hSVIP* gut OE (n=14 worms) worms (p-values indicated on graph). **c.** Gut-expressed SQST-1::mCherry::GFP in fed adult day 2 WT, *dSVIP* gut OE, and *hSVIP* gut OE worms (scale bar, 100µm). **d.** GFP/mCherry ratio in fed adult day 2 WT (n=11 worms), *dSVIP* gut OE (n=13 worms), and *hSVIP* gut OE (n=15 worms) worms (p-values indicated on graph). **e.** Gut-expressed Q64::YFP in fed adult day 1 WT, *dSVIP* gut OE, and *hSVIP* gut OE (scale bar, 100µm). **f.** Number of Q64::YFP aggregates in fed adult WT, *dSVIP* gut OE, and *hSVIP* gut OE worms on day 1 of adulthood (n=10 for each genotype; p-values indicated on graph). **g.** Thrashing rate of fed adult WT, *dSVIP* gut OE, and *hSVIP* gut OE worms (n=10 worms for each genotype; p-values on graph are comparisons to WT, **p<0.01, ***p<0.001, ****p<0.0001). **h.** Lifespan of fed adult WT, *dSVIP* gut OE, and *hSVIP* gut OE worms. **i.** Descriptive statistics for the lifespan comparison in Fig. 1h. **j.** Log-rank test results for lifespan comparisons in Fig. 1h.

Description

Small VCP Interacting Protein (SVIP) was first described as an endogenous inhibitor of Endoplasmic Reticulum-Associated Degradation (Ballar et al., 2007). Further work showed that SVIP recruits Valosin-Containing Protein (VCP) to lysosomes and is an essential protein for maintaining tubular lysosomal dynamic stability and autophagosomal-lysosomal fusion in *Drosophila* (Johnson et al., 2021; Johnson et al., 2015; Wang et al., 2011). Additionally, overexpression of *SVIP* in *Drosophila* muscles causes an increase in tubular lysosome (TL) density (Johnson et al., 2021). Significantly, TL induction correlates with improved animal health, and TL dysfunction has been linked to *VCP*-dependent diseases, underscoring the potential biomedical relevance of *SVIP* genes (Villalobos et al., 2023; Wall et al., 2021).

There is no known *SVIP* ortholog present in the *Caenorhabditis elegans* genome; however, our lab previously generated a transgenic *C. elegans* strain that expresses a codon-optimized *Drosophila* *SVIP* gene (*dSVIP*) in the gut (Villalobos et al., 2023). Although TLs are generally only stimulated in the gut of young-adult *C. elegans* under conditions of food limitation (Bohnert & Johnson, 2022; Dolese et al., 2022; Ramos et al., 2022), expression of *dSVIP* in the gut was sufficient to induce gut TLs constitutively and heighten autophagic activity in young-adult, well-fed *C. elegans* (Ricaurte-Perez et al., 2024; Villalobos et al., 2023). The human genome encodes an *SVIP* ortholog (*hSVIP*), which has not been previously characterized in any animal model. In this study, we created a transgenic *C. elegans* strain that overexpresses a full-length codon-optimized human *SVIP* transgene in the gut and assessed its effect on TL induction, autophagic activity, lifespan, and healthspan. The purpose of this study was to determine if human *SVIP* has similar phenotypic and physiological effects as *Drosophila* *SVIP*.

To determine if human *SVIP* overexpression stimulates TL formation constitutively, we overexpressed *hSVIP* in the gut of a strain expressing the lysosomal membrane protein SPIN-1 endogenously tagged with mCherry. Subsequently, we imaged SPIN-1::mCherry in fed day 1 adults, a condition in which TLs are not normally induced (Villalobos et al., 2023). While TLs were not robustly observed in young well-fed wildtype animals, overexpression of human *SVIP* induced constitutive TLs to a similar degree as overexpression of *Drosophila* *SVIP* (**Figure 1a-b**). Next, we determined if gut *hSVIP* overexpression heightened autophagic activity as we observed previously with the *Drosophila* ortholog (Villalobos et al., 2023). To do this, we imaged the autophagy receptor, SQST-1, tandemly tagged with mCherry and GFP (SQST-1::mCherry::GFP) (Villalobos et al., 2023). This autophagy reporter relies on the principle that GFP fluorescence is sensitive to the acidity in the lysosomal lumen, while mCherry fluorescence is unaffected by the low pH environment (Klionsky et al., 2021). Hence, low GFP fluorescence is indicative of more autophagic turnover. We imaged SQST-1::mCherry::GFP in the intestine of fed day 2 adults overexpressing human or *Drosophila* *SVIP* and compared autophagic turnover by quantifying the GFP/mCherry ratio. Overexpression of human *SVIP* in the gut decreased GFP fluorescence relative to control animals but not to the same extent as gut *dSVIP* overexpression (Figure **1c-d**). Thus, human *SVIP* overexpression increases autophagic activity but not as strongly as the *Drosophila* transgene. Similarly, it has been shown that expression of *Drosophila* *SVIP* suppresses protein aggregation, and we were curious if the human transgene would do the same. To do this, we expressed the aggregation-prone protein Q64 (Morley et al., 2002) tagged with yellow fluorescent protein (YFP) in the gut and imaged fed day 1 adults. Indeed, human *SVIP* reduced protein aggregates in day 1 adults relative to control animals but again not to the same degree as the *Drosophila* *SVIP* transgene (Figure **1e-f**). Thus, human *SVIP* overexpression heightens autophagic activity but not as strongly as *Drosophila* *SVIP*.

Next, we explored the physiological effects of human *SVIP* overexpression in the gut. It has been shown previously that expression of *Drosophila* *SVIP* in *C. elegans* improves healthspan independently of lifespan thereby decreasing the healthspan/lifespan gap (Villalobos et al., 2023). We found that expression of human *SVIP* exhibited a comparable improvement in late age mobility, a strong proxy for healthspan (Hahm et al., 2015), and had only a small effect on lifespan (Figure **1g-i**). Thus, expression of human *SVIP* promotes healthy aging and increases healthspan similar to expression of the *Drosophila* *SVIP* gene.

Collectively, we found that the human *SVIP* transgene causes similar phenotypic and physiological effects as the *Drosophila* transgene. Both transgenes induced TLs, heightened autophagic activity, and increased healthspan. Interestingly, while human *SVIP* did not increase autophagic activity to the same extent as *Drosophila SVIP*, there was minimal difference in physiological effects between these two strains. Potentially, this could indicate that the maximum autophagic activity triggered by the *Drosophila* gene is not required to achieve the maximum physiological effects. Future comparative studies on other *SVIP* orthologs could be informative to designing synthetic SVIP peptides that would maximize the therapeutic potential of SVIP-based strategies aimed at improving healthy aging or combating age-related diseases.

Methods

Animal maintenance

C. elegans were raised at 20ºC on Nematode Growth Medium (NGM) agar (51.3 mM NaCl, 0.25% peptone, 1.7% agar, 1 mM $CaCl_2$, 1 mM $MgSO_4$, 25 mM KPO_4, 12.9 µM cholesterol, pH 6.0) that were seeded with *E. coli* OP50 bacteria. Worms were synchronized by bleaching. Briefly, gravid hermaphrodites were vortexed in 1-2 mL bleaching solution (0.5 M NaOH, 20% bleach) for 3-5 minutes to isolate eggs, and eggs were washed three times in M9 buffer (22 mM KH_2PO_4, 42 mM Na_2HPO_4, 85.5 mM NaCl, 1 mM $MgSO_4$) before plating on NGM plates seeded with OP50 bacteria. In all aging experiments, including the lifespan assay, adult worms were picked onto fresh OP50-seeded NGM plates every day to separate adults from progeny.

Transgenic strain generation

All strains used in this study were generated using standard genetic crosses or microinjection. For genetic crosses, transgenes expressing fluorescent proteins were tracked by stereomicroscopy. For microinjection, constructs were injected individually or in combination into the gonad of adult hermaphrodites, each at a concentration of 25 ng/µl. Integration of transgenes was achieved using UV irradiation, followed by >5 generations of outcrossing. The *dSVIP* transgene was generated in a previous study (Villalobos et al., 2023), and the *hSVIP* transgene was generated as follows:

P*ges-1::hSVIP::unc-54 UTR:*

The coding sequence for human *SVIP* was codon-optimized for *C. elegans* expression using the *C. elegans* Codon Adaptor (Redemann et al., 2011). This sequence, flanked by a 5' attB1 and a 3' attB2 sequence, was then synthesized as a gBlock by Integrated DNA Technologies:

GGGGACAAGTTTGTACAAAAAAGCAGGCTCAAAAaaaaATGGGGTTGTGTTTTCCTTG
TCCGGGTGAGTCTGCTCCTCCAACCCCAGATCTTGAGGAGAAGCGGCTAAGCTCGCTGAG
GCCGCTGAGCGCCGTCAAAAGGAGGCCGCTTCCCGTGGAATCCTTGACGTCCAATCCGTT
CAAGAGAAGCGCAAGAAGAAGGAGAAGATCGAGAAGCAAATCGCCACTTCTGGTCCACCA
CCAGAGGGAGGACTCCGTTGGACCGTCTCCTAAACCCAGCTTTCTTGTACAAAGTGGTCCCC.

This *hSVIP* sequence was then cloned into the pDONR221 Gateway entry vector using BP clonase (ThermoFisher), and the insert was verified by DNA sequencing. Ultimately, pDONR221 *hSVIP* was combined with lab-stock plasmids pDONR P4-P1r P*ges-1* and pDONR P2R-P3 *unc-54* 3' UTR into the pDEST R4-R3 Gateway destination vector using LR clonase (ThermoFisher).

Microscopy methods

For *C. elegans* whole animal imaging, 4% agarose (Fisher Bioreagents) pads were dried on a Kimwipe (Kimtech) and then placed on top of a Gold Seal™ glass microscope slide (ThermoFisher Scientific). A small volume of 2 mM levamisole (Acros Organics) was spotted on the agarose pad. Worms were transferred to the levamisole spot, and a glass cover slip (Fisher Scientific) was placed on top to complete the mounting. Fluorescence microscopy was performed using a Leica DMi8 THUNDER imager, equipped with 10X (NA 0.32), 40X (NA 1.30), and 100X (NA 1.40) objectives and GFP and Texas Red filter sets.

Image analysis

Images were processed using LAS X software (Leica) and FIJI/ImageJ (NIH). Lysosome networks were analyzed using “Skeleton” analysis plugins in FIJI. Briefly, images were converted to binary 8-bit images and then to skeleton images using the “Skeletonize” plugin. Skeleton images were then quantified using the “Analyze Skeleton” plugin. Number of objects, number of junctions, and object lengths were scored. An “object” is defined by the Analyze Skeleton plugin as a branch connecting two endpoints, an endpoint and junction, or two junctions. Junctions/object was used as a parameter to quantify network integrity. For analyzing fluorescence intensity, the gut tissue was outlined using the free-draw tool in FIJI/ImageJ, and average fluorescence intensity of the outlined area was measured. For SQST-1::mCherry::GFP fluorescence ratio experiments,

50% laser intensity, 300 ms exposure time, and 100% Fluorescence Intensity Manager settings were used. For Q64 protein aggregate quantification, fluorescent aggregates were counted manually for each individual worm.

Thrashing and lifespan assays

Synchronous populations of animals were obtained by bleaching gravid adults (see animal maintenance), and worms in the late L4 larval stage were transferred to NGM plates seeded with OP50 bacteria. Throughout both assays, adult worms were transferred to fresh plates every day (to separate adults from their progeny) until reproduction ceased. For thrashing assays, individual worms were transferred into a drop of M9 buffer on an NGM plate, and the number of body bends were counted in a 1-minute period. For lifespans, dead worms were scored every 1-3 days. Worms that exploded, bagged, or crawled off plates were censored during analysis. Lifespans were analyzed using OASIS 2 software (Han et al., 2016), and statistical significance was assessed using a log-rank test.

Statistical Analyses

Data were statistically analyzed using GraphPad Prism. For all experiments, data distribution was assumed to be normal, but this was not formally tested. For three sample comparisons, a one-way analysis of variance (ANOVA) with Tukey's multiple comparisons was used to determine significance ($\alpha = 0.05$). For grouped comparisons, a two-way ANOVA with Šídák's multiple comparisons was used to determine significance ($\alpha = 0.05$). Statistical significance of lifespan data was determined using a log-rank test.

Reagents

Strain name	Genotype	Source
Bristol N2	Wild type	Lab stock
COP2331	*spin-1(knu1010[spin-1::mCherry::loxP::HygR::loxP]) V*	Villalobos et al., 2023 (by *In Vivo* Biosystems)
KAB58	*louIs5(Pges-1::dSVIP::unc-54 UTR + Podr-1::rfp) III*	Villalobos et al., 2023
KAB62	*louIs5(Pges-1::dSVIP::unc-54 UTR + Podr-1::rfp) III*; *spin-1(knu1010[spin-1::mCherry::loxP::HygR::loxP]) V*	Villalobos et al., 2023
KAB111	*louIs7(Pges-1::sqst-1::mCherry::gfp::unc-54 UTR) IV*	Villalobos et al., 2023
KAB143	*louIs5(Pges-1::dSVIP::unc-54 UTR + Podr-1::rfp) III;* *louIs7(Pges-1::sqst-1::mCherry::gfp::unc-54 UTR) IV*	Villalobos et al., 2023
KAB162	*louIs11(Pvha-6::Q64::YFP + rol-6(su1006))*	This study
KAB170	*louIs13(Pges-1::hSVIP::unc-54 UTR + Podr-1::rfp)*	This study
KAB269	*louIs7(Pges-1::sqst-1::mCherry::gfp::unc-54 UTR) IV; louIs13(Pges-1::hSVIP::unc-54 UTR + Podr-1::rfp)*	This study

KAB281	*spin-1(knu1010[spin-1::mCherry::loxP::HygR::loxP]) V; louIs13(Pges-1::hSVIP::unc-54 UTR + Podr-1::rfp)*	This study
KAB282	*louIs11(Pvha-6::Q64::YFP + rol-6(su1006));* *louIs13(Pges-1::hSVIP::unc-54 UTR + Podr-1::rfp)*	This study
KAB341	*louIs5(Pges-1::dSVIP::unc-54 UTR + Podr-1::rfp) III;* *louIs11(Pvha-6::Q64::YFP + rol-6(su1006))*	This study

Acknowledgements:

The authors thank all members of the Bohnert and Johnson labs for helpful discussions on this project.

References

Ballar P, Zhong Y, Nagahama M, Tagaya M, Shen Y, Fang S. 2007. Identification of SVIP as an endogenous inhibitor of endoplasmic reticulum-associated degradation. J Biol Chem 282(47): 33908-14. PubMed ID: 17872946

Bohnert KA, Johnson AE. 2022. Branching Off: New Insight Into Lysosomes as Tubular Organelles. Front Cell Dev Biol 10: 863922. PubMed ID: 35646899

Hahm JH, Kim S, DiLoreto R, Shi C, Lee SJ, Murphy CT, Nam HG. 2015. C. elegans maximum velocity correlates with healthspan and is maintained in worms with an insulin receptor mutation. Nat Commun 6: 8919. PubMed ID: 26586186

Han SK, Lee D, Lee H, Kim D, Son HG, Yang JS, Lee SV, Kim S. 2016. OASIS 2: online application for survival analysis 2 with features for the analysis of maximal lifespan and healthspan in aging research. Oncotarget 7(35): 56147-56152. PubMed ID: 27528229

Johnson AE, Orr BO, Fetter RD, Moughamian AJ, Primeaux LA, Geier EG, et al., Davis GW. 2021. SVIP is a molecular determinant of lysosomal dynamic stability, neurodegeneration and lifespan. Nat Commun 12(1): 513. PubMed ID: 33479240

Johnson AE, Shu H, Hauswirth AG, Tong A, Davis GW. 2015. VCP-dependent muscle degeneration is linked to defects in a dynamic tubular lysosomal network in vivo. Elife 4. PubMed ID: 26167652

Klionsky DJ, Abdel-Aziz AK, Abdelfatah S, Abdellatif M, Abdoli A, Abel S, et al., Tong CK. 2021. Guidelines for the use and interpretation of assays for monitoring autophagy (4th edition)(1). Autophagy 17(1): 1-382. PubMed ID: 33634751

Morley JF, Brignull HR, Weyers JJ, Morimoto RI. 2002. The threshold for polyglutamine-expansion protein aggregation and cellular toxicity is dynamic and influenced by aging in Caenorhabditis elegans. Proc Natl Acad Sci U S A 99(16): 10417-22. PubMed ID: 12122205

Ramos CD, Bohnert KA, Johnson AE. 2022. Reproductive tradeoffs govern sexually dimorphic tubular lysosome induction in Caenorhabditis elegans. J Exp Biol 225(12). PubMed ID: 35620964

Redemann S, Schloissnig S, Ernst S, Pozniakowsky A, Ayloo S, Hyman AA, Bringmann H. 2011. Codon adaptation-based control of protein expression in C. elegans. Nat Methods 8(3): 250-2. PubMed ID: 21278743

Johnson A, Ricaurte-Perez C, Wall P, Dubuisson O, Bohnert K. 2024. DAF-16/FOXO and HLH-30/TFEB comprise a cooperative regulatory axis controlling tubular lysosome induction in C. elegans. Res Sq. PubMed ID: 38585786

Villalobos TV, Ghosh B, DeLeo KR, Alam S, Ricaurte-Perez C, Wang A, et al., Johnson AE. 2023. Tubular lysosome induction couples animal starvation to healthy aging. Nat Aging 3(9): 1091-1106. PubMed ID: 37580394

Wall JM, Basu A, Zunica ERM, Dubuisson OS, Pergola K, Broussard JP, et al., Johnson AE. 2021. CRISPR/Cas9-engineered Drosophila knock-in models to study VCP diseases. Dis Model Mech 14(7). PubMed ID: 34160014

11/1/2024 - *Open Access*

Wang Y, Ballar P, Zhong Y, Zhang X, Liu C, Zhang YJ, et al., Fang S. 2011. SVIP induces localization of p97/VCP to the plasma and lysosomal membranes and regulates autophagy. PLoS One 6(8): e24478. PubMed ID: 21909394

Funding:

Funding for this project comes from the W.M. Keck Foundation (KAB, AEJ) and the National Institutes of Health grants R35GM138116 (AEJ) and R01AG079970 (KAB).

Supported by National Institutes of Health (United States) R35GM138116 to Alyssa Johnson.

Supported by W. M. Keck Foundation (United States) to Alyssa Johnson and K. Adam Bohnert.

Supported by National Institutes of Health (United States) R01AG079970 to Kenneth Adam Bohnert.

Author Contributions: Joshua P. Gill: data curation, formal analysis, investigation, writing - original draft, writing - review editing. Kathryn R. DeLeo: writing - review editing, resources, methodology. K. Adam Bohnert: writing - review editing, funding acquisition, conceptualization, supervision. Alyssa E. Johnson: conceptualization, funding acquisition, supervision, writing - original draft, writing - review editing, visualization, project administration.

Reviewed By: William Mair

Nomenclature Validated By: Anonymous

WormBase Paper ID: WBPaper00067421

History: Received October 1, 2024 **Revision Received** October 28, 2024 **Accepted** October 31, 2024 **Published Online** November 1, 2024 **Indexed** November 15, 2024

Citation: Gill, JP; DeLeo, KR; Bohnert, KA; Johnson, AE (2024). Human *SVIP* is sufficient to stimulate tubular lysosomes and extend healthspan in well-fed *Caenorhabditis elegans*. microPublication Biology. 10.17912/micropub.biology.001379